Contents lists available at *Dergipark*

Journal of Scientific Reports-A

journal homepage: *https://dergipark.org.tr/tr/pub/jsr-a*

E-ISSN: 2687-6167 ***Number 57, June 2024***

RESEARCH ARTICLE

Receive Date: 04.03.2024 *Accepted Date: 15.04.2024*

Tribological and mechanical performance evaluation of hybrid reinforced copper composites

Esad Kaya[a], Pelin Çağım Tokat-Birgin[b]*

[a] *Eskişehir Osmangazi University, Department of Mechanical Engineering, Eskişehir, Türkiye, ORCID: 0000-0002-7332-6154*

[b] *Kütahya Dumlupınar University, Department of Metallurgy and Material Engineering, Kütahya, Türkiye, ORCID: 0000-0001-9806-3381*

Abstract

The powder metallurgy technique is utilized in this study to produce Cu matrix hybrid composites with ZrO_2 reinforcements and graphite additives. This study compares composites' microstructural (theoretical, experimental, and relative density, phase morphology, type, chemical content), mechanical (microhardness), and tribological behavior (wear and friction) with 5, 10, and 15 wt% reinforcement, together with and without the effect of 2 wt% graphite additives. Homogenously ZrO_2 added copper alloy was successfully produced. All samples were produced at least %90 relative density. The XRD analyses also validate the phase presence of reinforcement phase. Also the graphite was added to samples which provides self-lubrication. The graphite addition improves friction behaviour. The hardness of the composites increased as the amount of ZrO_2 increased with the addition of graphite. The wear resistance of ZrO_2-added copper samples was improved between 1.32 and 4.84 times better than that of copper without reinforcement.

Keywords: Powder metallurgy, Metal matrix composites; Wear resistance; Friction

1. Introduction

Copper matrix composites have had many uses in recent years due to their superior mechanical, physical, and chemical properties [1]. Copper matrix composites are produced by adding many different reinforcement elements. Some of these are SiC [1], Al_2O_3 [2], MgO [3], and graphite composites [4]. Due to their superior thermal and electrical conductivity, copper-based metal matrix composites are very popular in the electrical and electronics industry [4]. Different carbide and oxide structures are used as reinforcement to improve both thermal and

mechanical properties [2]. Today, Cu-based composites manufacture brushes widely used in automotive applications such as door locks, starter motors, and blower motors [5-7]. As can be seen, the components mentioned are machine parts that operate at high speed and are subject to friction and wear. In the literature, the benefits of oxides integrated to the Cu structure have been revealed by different studies. Alumina particles have special qualities when distributed throughout the copper matrix, including potent strength, outstanding resistance to annealing, and high electrical and thermal conductivity. A study used the traditional and spark plasma sintering methods to generate an Al_2O_3-reinforced copper matrix in three distinct atmospheres: argon, nitrogen, and hydrogen. Using a hydrogen atmosphere, an issue of weak interfacial bonding in the nitrogen and argon atmosphere has been partially resolved. EDS analysis validates the same problem as well. The degree of bonding deteriorated during sintering in nitrogen and argon atmosphere due to the formation of Cu_2O [2]. Improvements in the Cu–Al_2O_3 system's compressive strength, hardness, and wear resistance were demonstrated by Fathy et al. [8]. A comparison was made between Cu–Al_2O_3 and copper alloy's wear resistance, and it was observed that the copper alloy without Al_2O_3 had the lowest wear resistance. Furthermore, it has been found that wear resistance increases with an increase in the Al_2O_3 ratio. The copper matrix composite samples with 2.5%, 7.5%, and 12.5% Al_2O_3 possess the following relative densities, in that order: 92%, 90%, and 88%. It is observed that the relative density is highest in pure copper alloy and lower in copper composites containing Al_2O_3, and this decrease continues as the additive ratio increases. It was determined that Brinell hardness values increased with increasing Al_2O_3 ratio. The hardness value of the pure copper alloy is 53.7HB, and the hardness of the copper matrix composite samples containing 2.5%, 7.5%, and 12.5% Al_2O_3 are 59.8HB, 67.9HB, and 79.4HB.

Due to its unique characteristics, which include high hardness, low coefficient of friction (COF), high elastic modulus, chemical inertness, and high melting point, zirconia is a ceramic material with a wide range of applications [9]. Studies using copper matrix composite materials with different reinforcements, including SiC, Y_2O_3, and TiO_2, have been published in the literature [1-4, 10, 11]. These reinforcements have significantly increased the hardness values of composite materials. Nevertheless, a literature review reveals that adding graphite to copper matrix composites increases their ability to resist friction and wear. [12, 13]. Studies have shown that graphite additive in Cu matrix composites reduces the alloy's hardness and increase wear resistance by acting as a solid lubricant. Based on this situation, the hardness of the composite samples is predicted to be increased by adding reinforcements such as ZrO_2 into the copper matrix. At the same time, the wear resistance of the samples was increasedy adding 2-3% graphite by volume. The samples were made using and without the addition of ceramic reinforcement-graphite addition. The effect of graphite and ceramic additives on microstructural (SEM-EDS and XRD analysis), tribological (wear rate, friction coefficient behavior), and mechanical (hardness) performance was investigated and relatively compared.

2. Material and method

Cu powder (NaNokar, 44 μm, 99.9%), ZrO_2 (Metco, 25 μm, 99.99%), and graphite (Alfa Easer, 44 μm, 99.5 %) were prepared according to calculated stoichiometric ratios. The starting powder materials were homogenized in 10 ml polyethylene containers for 12 hours at 150 rpm using a Retsch PM 400 planetary mill machine. The samples were pressed with a Calver manual press in a diameter of 1 cm. The shaped samples were pressurized to 200 MPa using a cold isostatic press (MSE-CIP) to make them more dense. In this study, the samples were produced utilizing a Protherm tube furnace operated in an argon atmosphere for two hours at 900 °C. The experimental densities of the samples were calculated using Archimedes' method [14]. PanAnalytical X-ray diffraction (XRD) was conducted at 30 kV and 30 mA with a Cu Kα radiation source. The FEI NovaNanoSEM650 scanning electron microscope (SEM) and the EDAX Trident energy scattering X-ray spectrometry (EDS) were used concurrently. The data regarding the microstructural characteristics and the location of the reinforcement (ZrO_2 and graphite) in the matrix (Cu) of the samples were gathered. The microhardness measurement technique was performed using Future Tech FM-800 equipment. Hardness evaluation tests were done at 25 gf load and 10 seconds of dwelling time. Also, the tribological

performance of all samples was evaluated. ASTM G99 test standard was used. The pin-on-disk type test method was selected and carried out in the CSM Tribometer device. A hardened 3 mm diameter 100Cr6 bearing steel ball was used as the counterbody. 3N was used as a test load. All wear tests were performed with a 6 mm diameter projectile circle. Wear test performed at 3 cm/sec (about @ 196 RPM). The total test distance was 50 meters. During the test, the COF was recorded instantly. In order to calculate the wear rate in a volumetric loss per load and distance, a cross-section of the worn surface was measured using a Mitutoyo SJ-400 surface roughness profilometer. Gaussian filtering techniques were used to determine of the average surface profile. Subsequently, after the wear test, SEM and EDS analyses were evaluated on the worn surfaces. The wear mechanism is characterized. The chemical composition of the produced samples were added to Table 1.

Table 1. The chemical composition of the produced samples.

Sample Code	Cu (% vol.)	ZrO_2 (%vol.)	Graphite(%vol.)
S-0	100	none	none
S-1	Balance	none	2
S-2	Balance	5	none
S-3	Balance	10	none
S-4	Balance	15	none
S-5	Balance	5	2
S-6	Balance	10	2
S-7	Balance	15	2

3. Result and discussion

The theoretical and relative densities of the samples were calculated, and experimental densities were measured. Density values are compared in Figure 1. The relative density of the copper sample S-0 is at its maximum compared to the other samples. Graphite and ceramic additives led to a decrease in the relative density. As the additional amount of ZrO_2 increases (S-2, S-3, and S-4, respectively), the relative density value is expected to decrease compared to other added compounds, while the relative densities of samples S-2 and S-3 are the same. In ceramic-reinforced metal matrix composites, 100% wetting between ceramic and metal may not be achieved. As ceramic reinforcement increases, the relative density of the composite may decrease. The relative densities of ZrO_2/graphite added copper matrix composite specimens are also expected to decrease with increasing ZrO_2 addition, while the relative density of specimen S-6 increased very slightly. S-7 showed a decrease, as expected. Considering the margins of error, there is no inconsistency in the result.

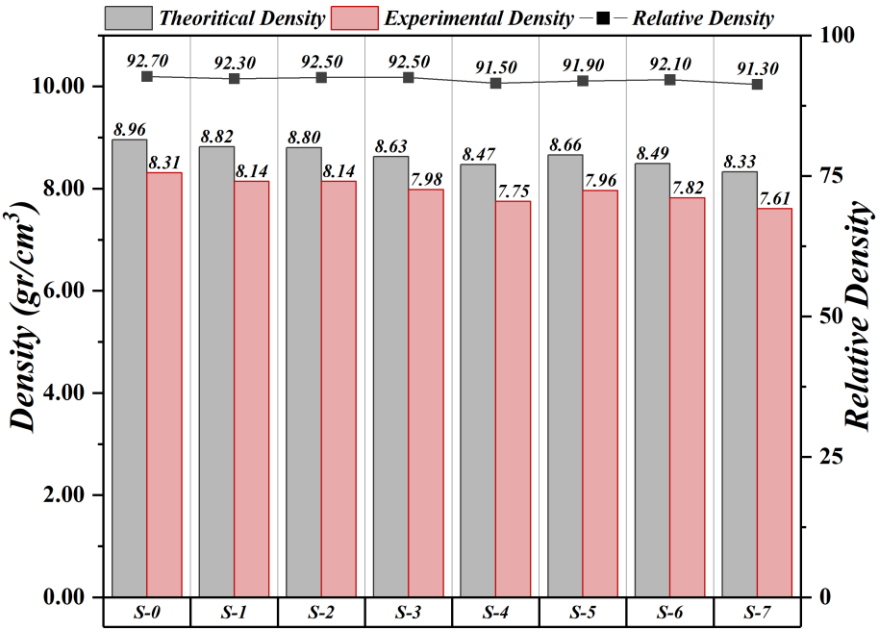

Fig. 1. Theoretical, experimental, and relative densities of ZrO_2 and ZrO_2/graphite added copper matrix composite samples.

Figure 2 shows SEM images of the composite samples. Figure 2a presents SEM images of the undoped sample, Figure 2b, 2c and 2d present SEM images of the samples containing 5%, 10% and 15% ZrO_2, respectively. The amount of ZrO_2 in the composites is directly proportional to the amount of ZrO_2 in the microstructures in the SEM images. In Figure 2b, the amount of ZrO_2 grains is relatively less, in Figure 2c it is slightly increased, and in Figure 2d it is slightly increased. The samples in Figure 2e, 2f, 2g, and 2h contain 2% graphite and 0%, 5%, 10% and 15% ZrO_2, respectively. Similar to the SEM images of the samples without graphite addition, as the amount of ZrO2 in the graphite and ZrO_2-added composites increased, the amount of ZrO_2 grains in the microstructures also increased (figures 2f, 2g and 2h, respectively). Figure 2e shows that the grain boundaries of the graphite-containing sample are more indistinct than in Figure 2a and that the graphite is homogeneously distributed in the copper matrix. In images b, c, f, and g, it is evident that the ZrO_2 grains retain their structural integrity. In the study by Elmahdy et al., It was mentioned that due to their high melting point, high hardness, exceptional thermal stability, and chemical inertness, ZrO_2 grains are present in the Cu matrix whereas no melting occurs. It was mentioned that the reinforcement grains increase the strength of the sample by preventing the movement of dislocations [15]. The SEM images obtained in the study are similar to those in the literature. It is clear from the microstructure analysis that the samples are sintered and well-densified.

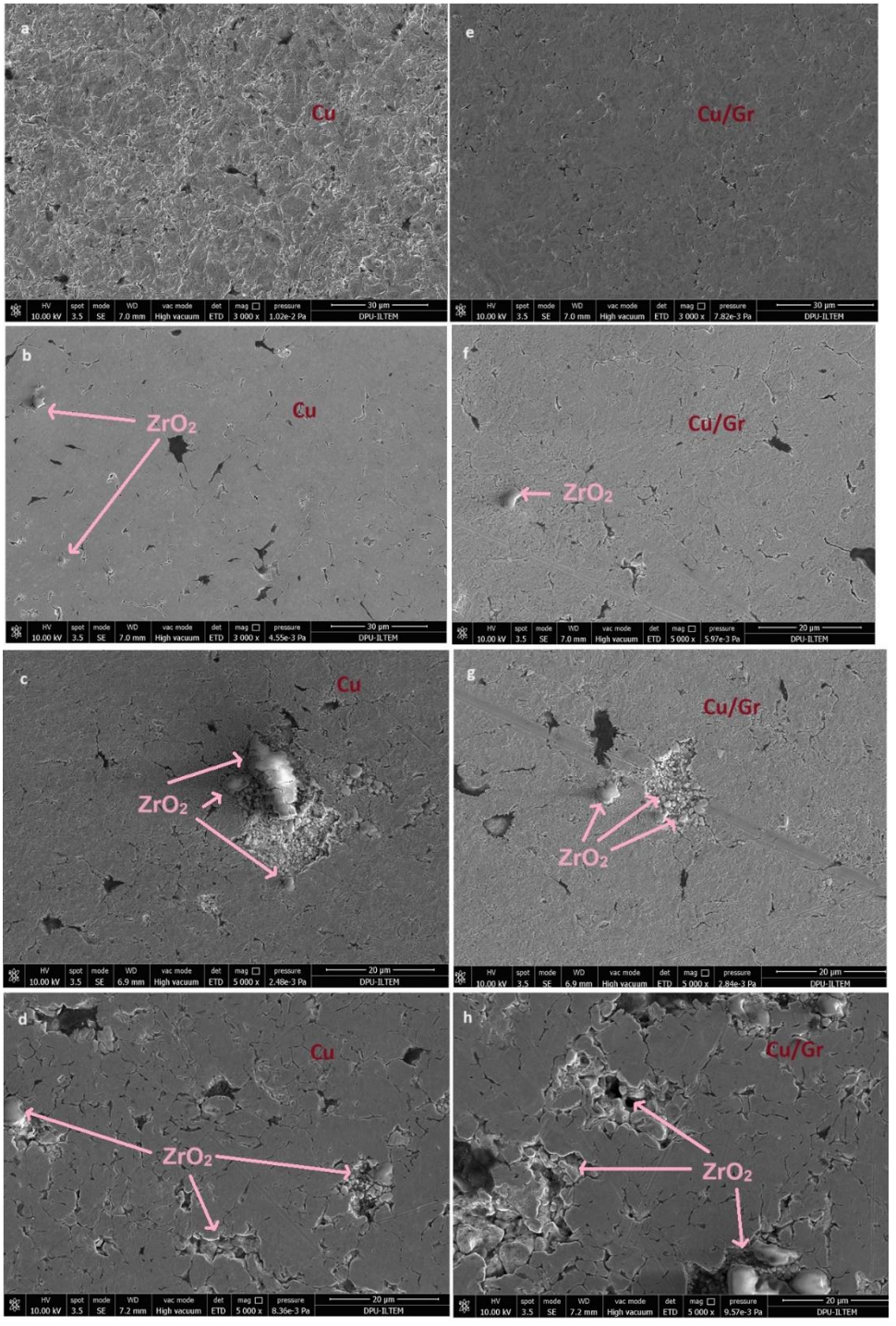

Fig. 2. SEM images of (a) S-0, (b) S-1, (c) S-2, (d) S-3, (e) S-4, (f) S-5, (g) S-6, (h) S-7.

Data from the SEM/EDX analysis in Figures 3a and 3b are shown. The principal Cu, C, O, and Zr peaks were found, which correspond to the ZrO_2 particle and Cu matrix compositions, respectively. For both samples, two spot analyses and one field analysis were performed. The peak intensities and numerical data obtained agree with the of stoichiometry composition.

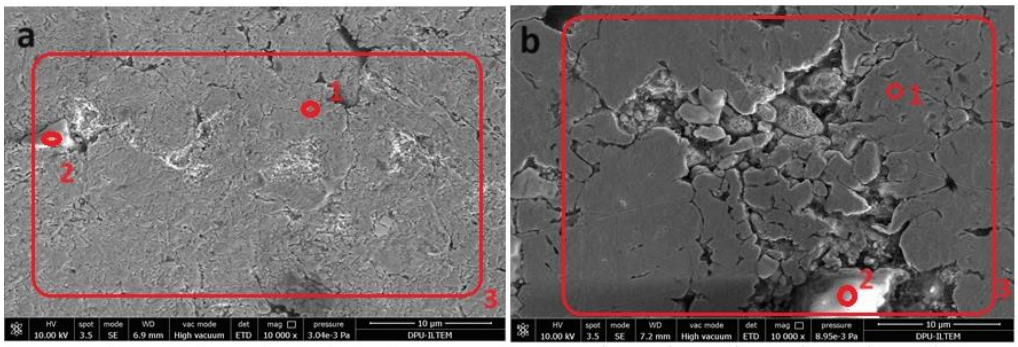

Element	Cu	Zr	O
Spot1	99,17	0,62	0,21
Spot2	32,94	48,93	18,13
Spot3	82,91	10,73	6,36

Element	Cu	Zr	O	C
Spot1	97,37	0,45	0,32	1,86
Spot2	21,93	56,37	20,28	1,42
Spot3	73,02	17,22	7,45	2,31

Fig. 1. SEM-EDX images of (a) S-4, (b) S-7 samples.

The field emission SEM micrograph and matching map analysis used to ascertain the distribution of the composite's elemental parts are displayed in Figure 4. The elemental components of the structure are distributed uniformly, according to the surface scan results. Nearly the entire surface is covered in copper and zirconium and are readily apparent at a particular location in the surface scan. A low level of carbon and oxygen content were also detected. The carbon content was detected as % 3.13. One can be infer that the low atomic diameter elements (such as C, B, and O) s are hard to detect precise exact chemical composition

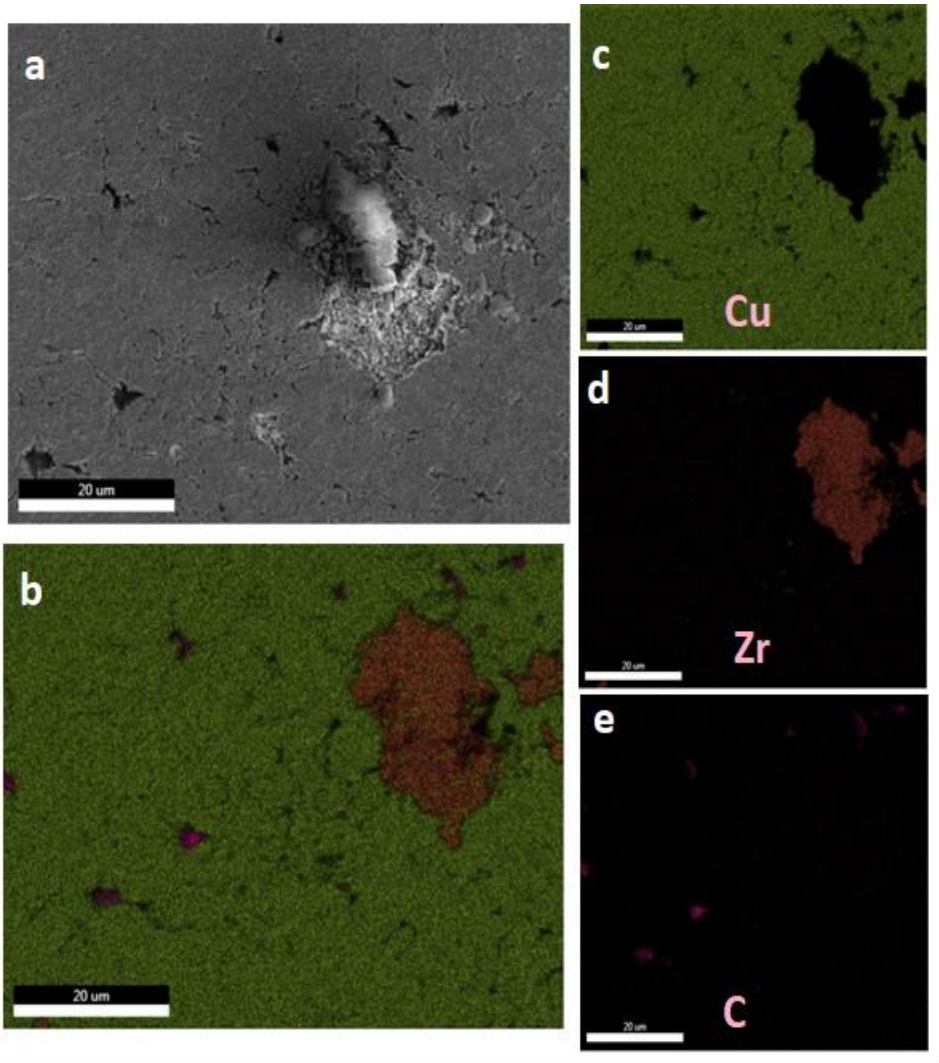

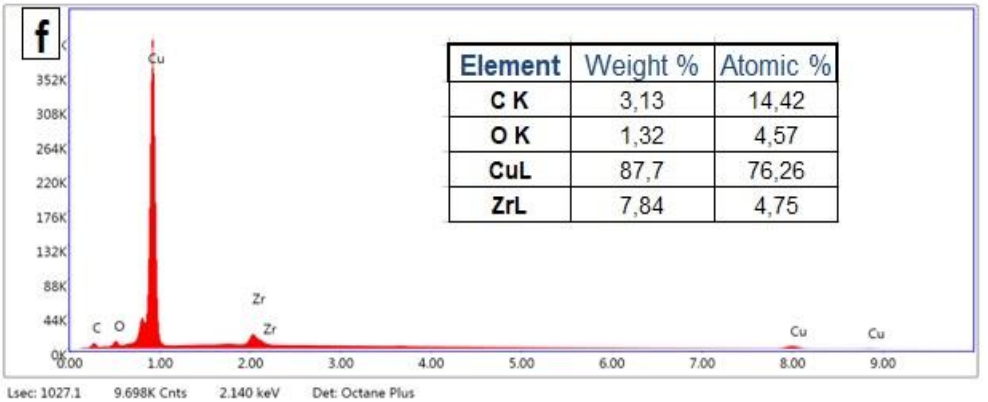

Element	Weight %	Atomic %
C K	3,13	14,42
O K	1,32	4,57
CuL	87,7	76,26
ZrL	7,84	4,75

Fig. 4. (a) SEM image of the sample S-7, (b) elemental mapping of sample S-7, (c) the element mapping of Cu in (a), (d) the element mapping of Zr in (a); (e)the element mapping of C in (a), (f) the element mapping spectrum of sample S-7.

The data obtained after X-ray diffraction (XRD) analysis of ZrO_2 and ZrO_2-graphite added copper matrix samples are shown in figures (a) and (b), respectively. For the ZrO_2-added samples, the primary phase is copper, and the peaks of the copper phase are observed at 2theta = 43.3°, 50.4°, and 74.7°, similar to the other reinforced samples. Sample Z-2 does not appear to have a 100% zirconia peak. All ZrO_2-containing samples, including sample Z-5 with the same ratio, have this peak and a minimal zirconia peak at 31.7. As the reinforcement addition of ZrO_2 increases, the peaks of the zirconia phase also increase minimally. Due to the high intensity of Cu peaks and low level of the graphite content, it is thought that the peak of graphite phases settled in the background in ZrO_2-graphite added copper matrix composites. The elements added below 2% could not be detected as they were below the detection limit of the XRD.

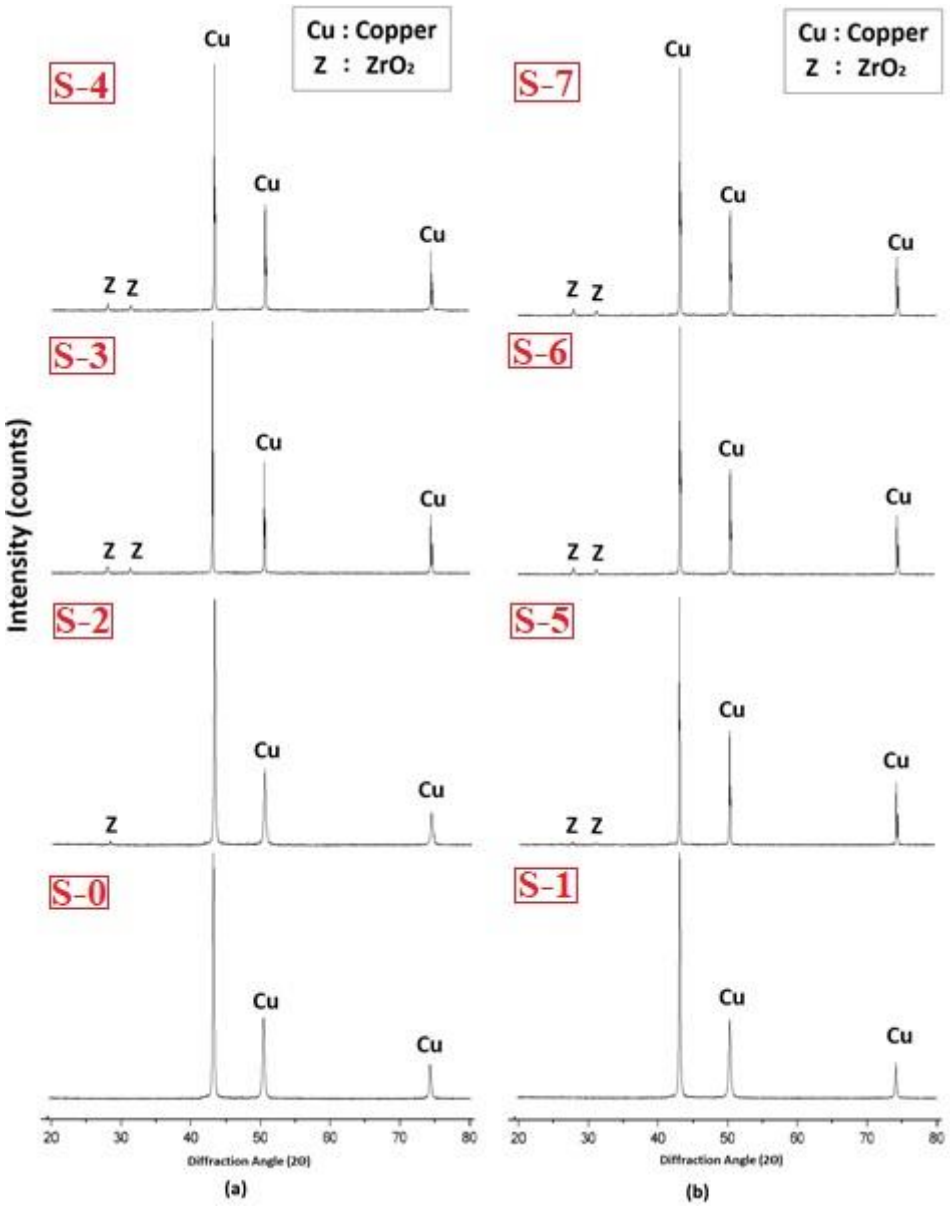

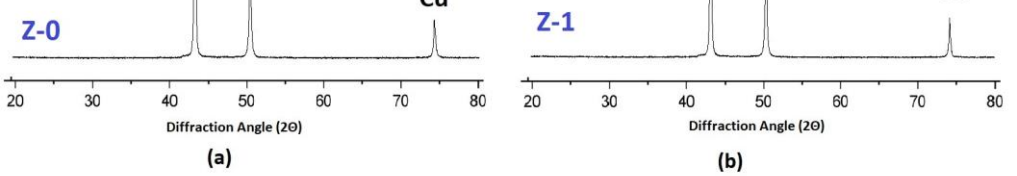

Figure 6 shows the microhardness properties of the produced samples. The lowest hardness was measured in S-0 sample which pure copper. The sample with graphite content (S-1) has a particularly lower hardness value than the pure copper sample (S-0). The main reason for this situation is graphite couldn't affinity to copper elements in the microstructure. When the ZrO_2 addition rate increases by 5%, 10%, and 15%, the hardness change increases significantly. As the amount of ZrO_2 increased, the hardness of the samples increased linearly as the reinforcement distribution incrase general stiffness was incrased. The hardness value of graphite/ZrO_2 added samples (S-5, S-6, and S-7) is higher than that of only ZrO_2 added (S-2, S-3 and S-4). The addition of graphite is increased general stiffness due to integration to grain boundaries. It is higher than the copper composite sample (S-1) containing only graphite.

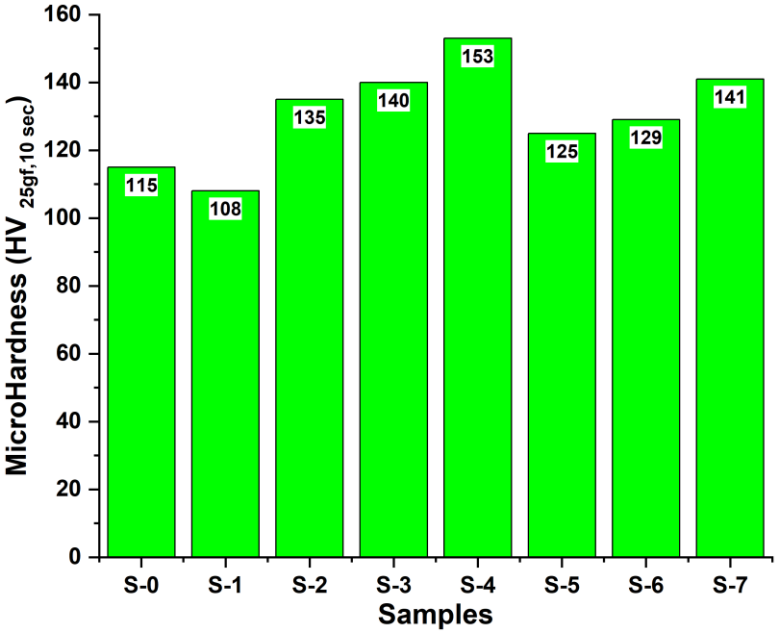

Fig. 6. Hardness of of ZrO_2 and ZrO_2/graphite added copper matrix composite samples.

Figure 7 shows the wear resistance-COF alteration graph of samples containing Cu matrix, ZrO_2 ceramic reinforcement phase, and Graphite additive at different rates. The diagram is reported as wear rate and average friction coefficient. Higher wear rates mean inferior wear resistance. Wear rates are calculated by taking the average value of the applied load, distance, wear scar diameter, and the resulting wear channel. Equation 1, given below, shows the formulation used in wear rates. D is the diameter of wear track that used in the test (mm), A is the surface cross section worn surface obtained by surface profilometer (mm^2), P is the normal load that used in the test (N), L is the wear test distance as meter.

$$Wear\ Rate = \left(\frac{\pi.D.A}{P.L}, \frac{mm^3}{N.m} \right) \quad (1)$$

As can be seen from the diagram, ceramic reinforcement added to the structure at different rates dramatically improves the wear resistance of the structure. Due to increased ceramic particle reinforcement, wear rates have significantly improved in all reinforced groups over and plain graphite-added Cu alloys. Wear performance improvements in samples produced by adding different amounts of ZrO_2 to the microstructure vary between %132 to%484 comparison to the lean Cu sample (S0). Only ZrO_2 reinforcements improve wear resistance %136 to %331. ZrO_2 reinforcement and the graphite addition improved the wear resistance %132 to %484. One can infer that combining oxide and graphite improve wear resistance more efficiently. However, adding lean graphite did not directly improve the wear resistance; on the contrary, it caused a decrease in the wear performance. When the wear rate and average friction coefficient of the lean graphite added sample (S-1) are examined, it is seen that it shows a high wear rate. However, this sample had the lowest friction coefficient among all groups. The friction coefficient is not an exact material property but the response of the created tribological coupled system. The friction coefficient graph of this sample is examined (Fig. 8), showing that the friction behavior is stable after 10 meters. The EDS analysis of the worn surface showed that the presence of oxide layers formed on the surface is seen. Wear increased with the first contact but decreased with increasing test distance due to graphite-based oxides formed on the direct metal-metal contact surfaces. The structure's absence of a hard reinforcement phase (such as ZrO_2 for this case) increased the actual contact area on the interface. Although graphite, known to be soft and able to move within its own layers, prevents direct metal-metal contact on surfaces, it does not directly affect wear resistance. Thus, the wear rate deteriorated. This situation is thought to be due to the formation of tertiary particles by graphite combining with O in the ambient atmosphere during the test. The resulting complex tribochemical oxides caused abrasive damage to the pure Cu matrix and caused worsening wear. Graphite is known to be an excellent solid lubricant with the ability to move through layers. For this reason, graphite plastered on the surfaces reduced the friction.

When the wear performances of ceramic particle-reinforced samples are compared to the reference sample, the wear rates are improved by approximately 1.36 to 4.84 times. Ceramic particles placed in the Cu matrix increased the load-carrying ability of the surface. Similarly, the increasing amount of ceramic particles within the structure had a linear effect on wear performance. Samples containing plain ceramic particles are coded as S-2, S-3, and S4, and with increasing amounts of ceramic additives, wear rates decreased, and wear resistance improved in all samples. In addition to ceramic additives, the effect of ceramic particles and graphite reinforcement on wear and friction was also examined in the experiments. For this reason, the wear behavior of samples containing graphite with different amounts of ceramic particle reinforcement was characterized using the same test parameters. These samples are coded as S-5, S-6, S-7. Graphite additives do not have the same effect in every ceramic particle system. Graphite content in ZrO_2-reinforced samples had a positive effect and reduced friction.

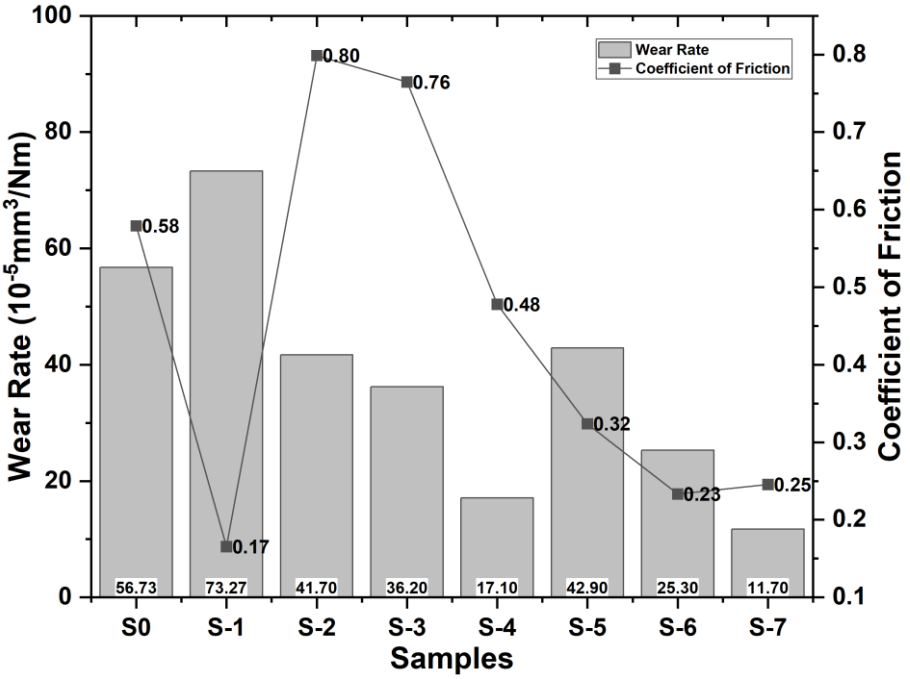

Fig. 7. The comparative wear rate of ceramic particle-reinforced alloy systems at different rates.

Figure 8 shows the distance-dependent COF alteration graphs of samples containing different ratios of ZrO_2 ceramic reinforcement phase and graphite additive. When the graphs are examined in general, it is seen that the friction behaviors enter a regular regime called the incubation period after passing the static friction point. Friction behavior in all samples showed stable behavior at the end of the test except for the S-6. This case indicates that the selected test distance is optimum for the specified load and speed values. S-2 sample which has contains lowest reinforcement ratio, exhibits higher steady regime comparison to other samples. A high friction regime was observed in the S-0 sample for the first 20 meters which is the reference sample. During the mid-regime of the test, the COF behavior getting stabilized. The situation shows that third bodies at the interfaces were extracted from the worn surfaces. Thus the COF behavior was stabilized with the help of copper-based oxides. Although sample S-1 has a high wear rate, it has a low COF—this situation affects the graphite present in the structure. Samples S-2, 3, and 4 are ceramic-added samples that do not contain graphite. As expected, the average COF behavior of these samples is higher than those containing graphite. Among the graphite-added samples, the system showing the highest oscillation is the S-5 and S-6. This situation develops due to oxides breaking and breaking with continuous contact at increasing wear test distance. Particles that break off and remain on the rubbing interface cause an increase in the friction force due to compression and cause fluctuations. Sample S-7 is the sample with the lowest wear rate. Similarly, it exhibited the relatively steady friction behavior in the ZrO_2-reinforced groups. High and hard ceramic grains in the microstructure reduced the deteriorating effects of the wear. It also reduced the COF by reducing the actual contact rate.

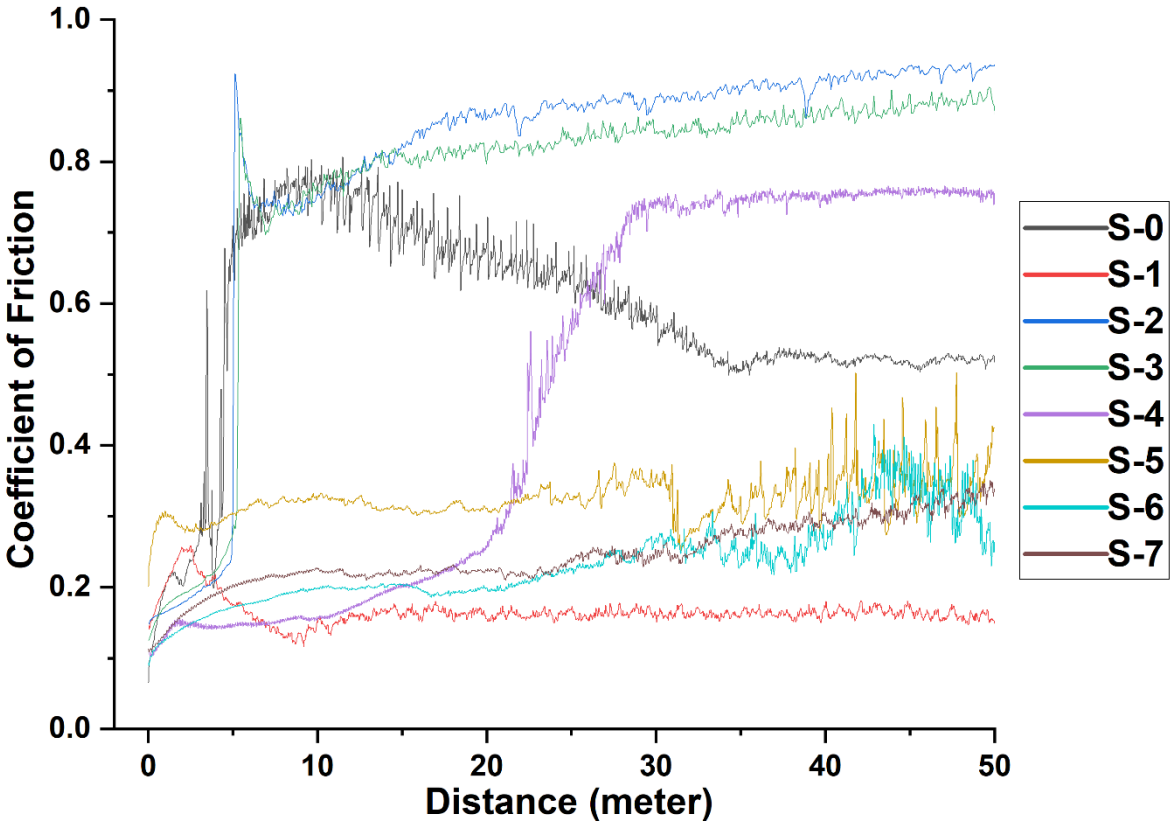

Fig. 8. The COF behavior is based on the distance of the samples.

Figure 9 shows the worn surface SEM-EDS analysis of the reference sample without additives (S-0) and the graphite-added sample (S-1). When the wear surface of the reference sample is examined, it is seen that the wear mechanism is primarily oxidative in places. These formed oxides are brittle and break at increasing wear distances. These broken pieces remained on the surface, allowing three-body abrasive wear to begin. Although the dominant wear mechanism in the reference sample is oxidative, abrasive effects are also observed. When the SEM-EDS analysis of the wear surface of the graphite-added reference sample is examined, it is clear that the wear mechanism is entirely abrasive. There is also superficial oxide formation on the surfaces. There is graphite found in the structure. Graphite incorporated into the structure is a type of solid lubricant and is one of the main topics known in the literature. The solid lubricity of graphite occurs due to the weak interlayer bonds. Graphite inside the microstructure is plastered on both surfaces. Graphite moving between layers after plastering ensured low friction on the surface. However, the absence of a reinforcement phase supporting the matrix within the structure poses a negative situation regarding load-bearing ability. With increasing wear test distances and wear load, also the plastic deformation mechanism of abrasive wear deformed the surface. For this reason, the wear performance of the plain graphite added sample performed weak weak wear resistance compared to the reference sample.

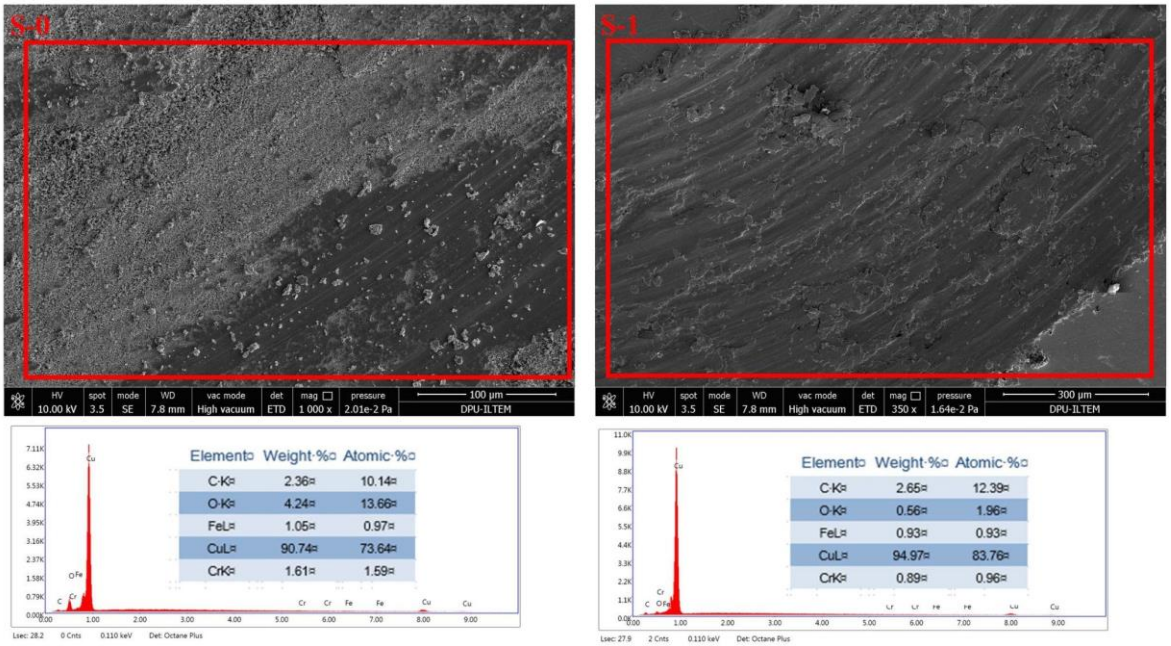

Fig. 9. Worn surface SEM-EDS analysis of reference sample (S-0) and graphite added sample (S-1).

SEM and EDS analyses of worn surfaces are shown in Figures 9, 10 and 11 respectively. Figure 9 exhibits SEM-EDS analysis of the worn surface of S-0 and S-1 which are lean copper and graphite added copper samples. Figure 10 and 11 shows SEM and EDS analyses of worn surface of different amounts of ZrO_2 reinforced samples. When the plain ceramic added group is examined, it is seen that the wear resistance is lower than the graphite added group. This sample group is the group characterized as having the lowest wear resistance. As can be seen, when the surfaces of these samples containing different amounts of ceramic reinforcement are examined, microcracks caused by contact are pretty visible. These microcracks occur after continuous contact with the high-hardness areas of both sides. It is a type of damage mechanism caused by surface fatigue. This situation indicates that the surface's load-bearing ability is low. Similarly, cleavages, indicators of brittle fracture, are frequently seen on the surfaces. In addition, despite the increased reinforcement ratio, oxidative wear on the surfaces was practical in all sample groups. The high wear appears to be three-body abrasive wear, which starts with oxidative origin and turns abrasive.

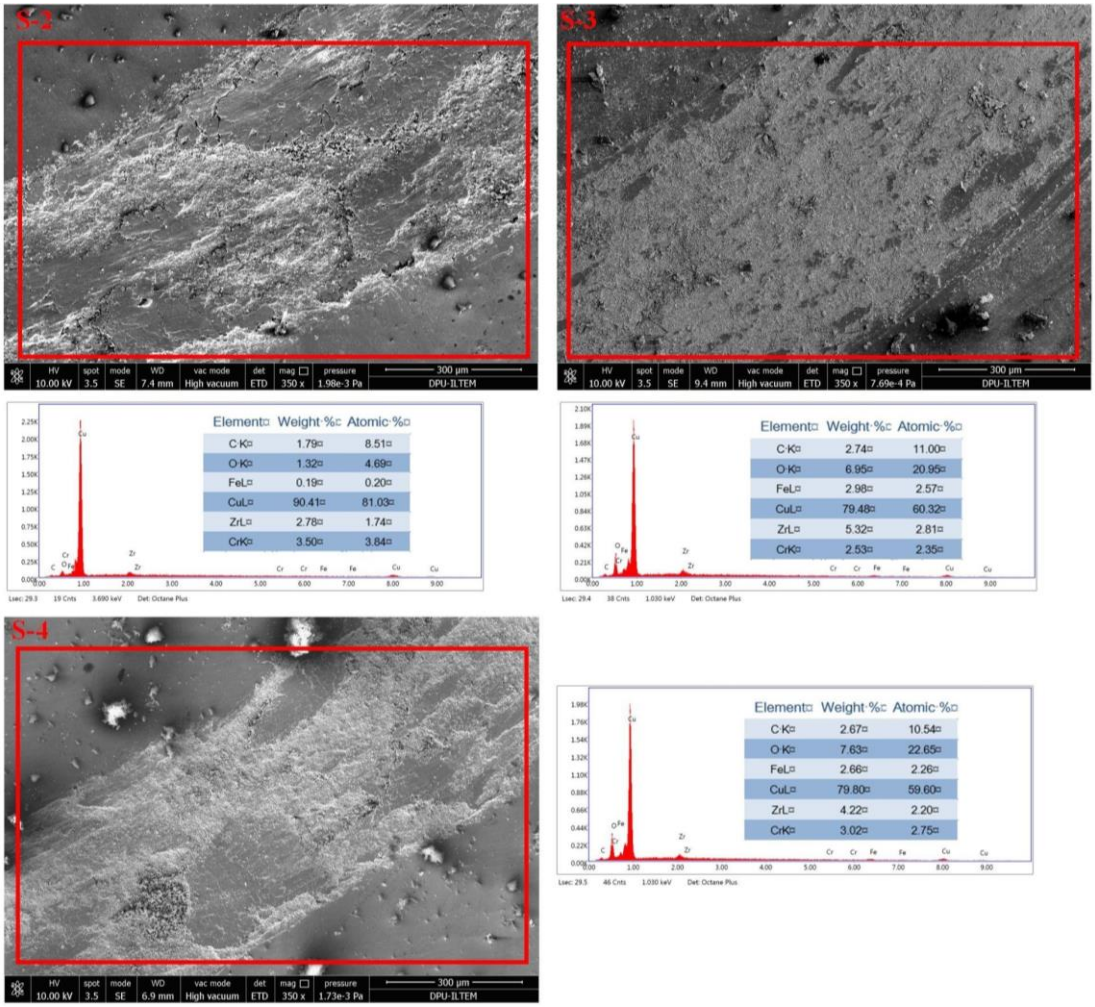

Fig. 10. Worn surface SEM and EDS analyses of samples containing different amounts of ZrO_2 additives.

The worn surface analysis photographs of both ceramic and graphite-added samples are given in Figure 11. Similarly, wear performance improved with increasing reinforcement ratio. The effect of graphite addition was observed very clearly in this alloy system. A decrease in the channel width was observed in all graphite-added samples. This situation is an indication that friction is decreasing. Surface damage in graphite-added ceramic particle-reinforced samples turned into an abrasive character. It is seen that the surface damage occurs superficially after increasing the reinforcement ratio. Increasing ceramic additive in the produced samples increased the probability of contact with the counter object, and wear decreased. Additionally, graphite smearing and interlayer movement reduced the actual contact zone and improved wear performance.

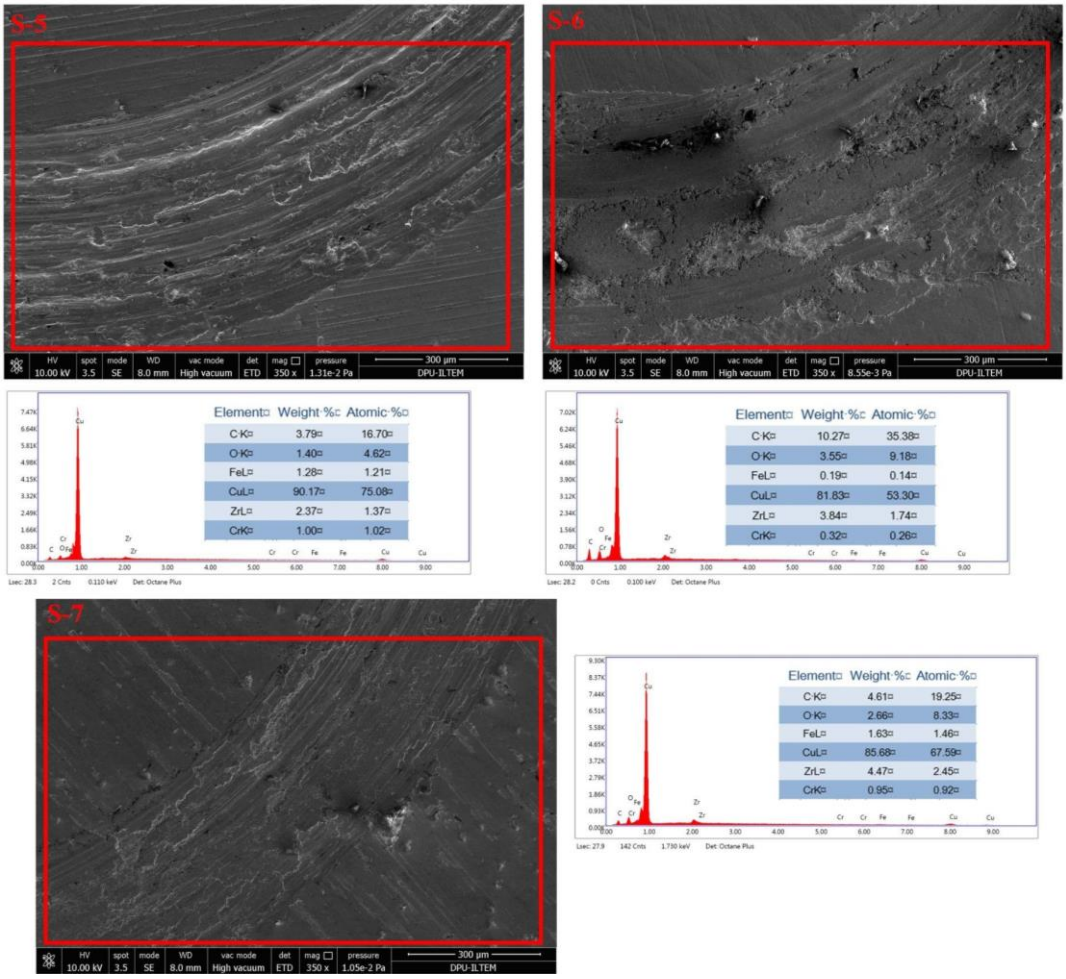

Fig. 11. Worn surface SEM and EDS analyses of samples containing different amounts of ZrO_2 and graphite.

4. Conclusions

Copper and copper matrix composites containing 5%, 10%, and 15% ZrO_2 by volume have been successfully produced via powder metallurgy. In addition to these samples, 2% graphite was added to each sample, and the mechanical properties of the samples were compared. Analysis and characterization methods such as XRD, theoretical, experimental, relative density, hardness, SEM, EDX, elemental EDX mapping, and wear were applied to the produced samples. If the results obtained are examined in detail, the following conclusions are drawn:

●When the theoretical, experimental, and relative densities of the produced Cu/ZrO_2 added and reference samples were compared, it was observed that the density values decreased with the addition of reinforcement. The average values of pure copper, ZrO_2, and both ZrO_2 and graphite-reinforced samples were 92.5%, 92.17%, and 91.77%, respectively. The relative densities of the specimens were found to be suitable by performing the specimens first and then cold isostatic pressing and pressing twice.

●As a result of the electron microscopy analysis, it was observed that the graphite was distrubuted in copper and homogeneously distributed. In contrast, in the samples containing ZrO_2, ZrO_2 was homogeneously distributed without dissolution, preserving the grain structure. The Cu, Zr, O, and C quantities obtained from the elemental analysis of the samples are consistent with each other and with the initial stoichiometries. Electron microscopy analysis supports the successful production of ZrO_2 and graphite reinforcements in all samples with homogeneous dispersion in the Cu matrix.

● XRD analysis shows that copper matrix composites containing ZrO_2 and copper matrix composites containing ZrO_2 and graphite were successfully fabricated.

● Samples with ZrO_2 reinforcement increased the hardness value considerably compared to the copper sample. Unsurprisingly, the hardness value of the samples containing 2% graphite additives increased, and the wear resistance decreased slightly compared to those without graphite.

● It has been observed that graphite additive positively affects wear resistance and friction behavior. No significant results regarding wear performance were obtained in the plain graphite additive sample.

● In samples containing graphite additives and ceramic additives, the coefficient of friction was reduced, and wear resistance was improved.

●With the study, the wear performance of Cu alloys was improved between 1.32 and 4.84 times. Wear resistance improved proportionally with increasing ceramic particle reinforcement.

●By evaluating microstructural, mechanical, and tribological properties, optimum chemical content was determined as %15 ZrO_2 reinforcement with the graphite additives. The material composition of S-7 sample could be utilized where wear resistance and friction behavior are important.

Conflicts of interest

The authors declare no conflicts of interest.

Acknowledgments

The Kutahya Dumlupınar University BAP (Scientific Research Project-Career Start Project) number 2022-32 provided funding for this work. For SEM, EDX, and mapping analysis, we are pleased to use the DPU-ILTEM (Kutahya Dumlupınar University-Advanced Technologies Research Center).

References

[1] F. Kennedy, A. Balbahadur, and D. Lashmore, "The friction and wear of Cu-based silicon carbide particulate metal matrix composites for brake applications," *Wear*, vol. 203, no. 5, pp. 715-721, March 1997, doi: 10.1016/S0043-1648(96)07384-X.

[2] K. Dash, B.C. Ray, and D. Chaira, "Synthesis and characterization of copper–alumina metal matrix composite by conventional and spark plasma sintering," *J. Alloys Compd.*, vol. 516, no. 1, pp. 78-84, March 2012, doi: 10.1016/j.jallcom.2011.11.136.

[3] X. Guo, K. Song, S. Liang, C. Zheng, "Thermal expansion behavior of MgO/Cu composite with lower MgO volume fraction," *Mater. Res. Bull*, vol. 47, no. 11, pp. 11-15, November 2012, doi: 10.1016/j.materresbull.2012.08.012.

[4] C. Samal, J. Parihar and D. Chaira, "The effect of milling and sintering techniques on mechanical properties of Cu–graphite metal matrix composite prepared by powder metallurgy route," *J. Alloys Compd.*, vol. 569, no. 1, pp. 95-101, August 2013, doi: 10.1016/j.jallcom.2013.03.122.

[5] J. Márquez, N. Antón, A. Jimenez , M. Madrid , M. Martinez, J. Bas, "Viability study and mechanical characterisation of copper–graphite electrical contacts produced by adhesive joining," *J. Mater. Process. Technol.*, vol. 143, no. 1, pp. 290-293, December 2003, doi : 10.1016/S0924-0136(03)00476-X.

[6] S. Hong, and B. Kim, "Fabrication of W–20 wt % Cu composite nanopowder and sintered alloy with high thermal conductivity," *Mater. Lett.*, vol. 57, no. 18, pp. 61-67, May 2003, doi: 10.1016/S0167-577X(03)00071-5.

[7] H. Mallikarjuna, C.S. Ramesh, P. Koppad, R. Keshavamurthy, D. Sethuram, "Nanoindentation and wear behaviour of copper based hybrid composites reinforced with SiC and MWCNTs synthesized by spark plasma sintering," *Vacuum*, vol. 145, no. 1, pp. 320-333, November 2017, doi: 10.1016/j.vacuum.2017.09.016.

[8] A. Fathy , F. Shehata, M. Abdelhameed, M. Elmahdy, "Compressive and wear resistance of nanometric alumina reinforced copper matrix composites," *Materials & Design*, vol. 36, no. 1, pp. 100-107, April 2012, doi: 10.1016/j.matdes.2011.10.021.
[9] M. Khaloobagheri, B. Janipour, and N. Askari, "Electrical and Mechanical Properties of Cu Matrix Nanocomposites Reinforced with Yttria-Stabilized Zirconia Particles Fabricated by Powder Metallurgy," *Adv. Mater. Res.*, vol. 829, no. 1, pp. 610-615, November 2013, doi: /10.4028/www.scientific.net/AMR.829.610.
[10] J. Mirazimi, P. Abachi, and K. Purazrang, "Spark Plasma Sintering of Ultrafine YSZ Reinforced Cu Matrix Functionally Graded Composite," *Acta Metall. Sin.*, vol. 29, no. 12, pp. 1169-1176, November 2016, doi: 10.1007/s40195-016-0512-0.
[11] Y. Qin, Y. Tian, Y. Zhuang, L. Luo, X. Zan, Y. Cheng, "Effects of solid–liquid doping and spark plasma sintering on the microstructure and mechanical properties of Y_2O_3-doped copper matrix composites," *Vacuum*, vol. 192, no. 110, pp. 436-445, October 2021, doi: 10.1016/j.vacuum.2021.110436
[12] H. Imai , Y. Kosaka, A. Kojima, S. L, K. Kondoh, J. Umeda, H. Atsumi, "Characteristics and machinability of lead-free P/M Cu60–Zn40 brass alloys dispersed with graphite," *Powder Technol.*, vol. 198, no. 3, p. 417-421, 2010, doi: 10.1016/j.powtec.2009.12.010.
[13] H. Imai, L. Shufeng, H. Atsumi, Y. Kosaka, A. Kojima, K. Kondoh, "Development of Lead-Free Machinable Brass with Bismuth and Graphite Particles by Powder Metallurgy Process," *Mater. Trans.*, vol. 51, no. 5, pp. 855-859, May 2010, doi: 10.2320/matertrans.MH200907.
[14] H. Aydin and P. Birgin, "Properties of Al/Al_2O_3-TiO_2 composites prepared by powder metallurgy processing," *Kovove Mater.*, vol. 59, no. 2, pp. 99-107, January 2021, doi: 10.4149/km 2021 2 99
[15] M. Elmahdy, G. Abouelmagd, A. Mazen, "Microstructure and properties of Cu-ZrO_2 nanocomposites synthesized by in situ processing," *Materials Research*, vol. 21, no. 1, pp. December 2018, doi: 10.1590/1980-5373-mr-2017-0387